Engineering Structures 309 (2024) 118054

Contents lists available at ScienceDirect

Engineering Structures

journal homepage: www.elsevier.com/locate/engstruct

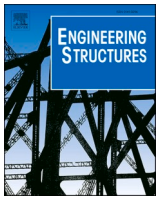

Experimental investigation on the flexural behavior of SFRC beams reinforced with hybrid reinforcement schemes

Ahmed El Bakzawy [a,*], Mohamed H. Makhlouf [b], T.S. Mustafa [a], Maher Adam [a]

[a] Civil Eng. Dept., Shoubra Faculty of Eng., Benha University, Egypt
[b] Civil Eng. Dept., Benha Faculty of Eng., Benha University, Egypt

ARTICLE INFO

Keywords:
Hybrid reinforcement
Steel fiber
RC beams
Flexural behaviors
Ductility
Nominal moment

ABSTRACT

Seven half-scale beams were tested to explore the impact of adding steel fiber (SF) on the flexural behavior of concrete beams reinforced with hybrid schemes. Key parameters included SF volume (0.00%, 0.50%, and 1.00%) and the steel-to-GFRP ratio in hybrid schemes (1.0 and 0.69). The presence of SF in the concrete beams, reinforced with hybrid schemes, enhances ductility while simultaneously increasing load capacity and stiffness. Load capacity increased by 13% and 21% for 0.50% and 1.00% SF, respectively. Toughness enhancements were 97.7% and 161% for the same SF volumes. SF presence led to higher strains in GFRP bars at ultimate levels, enhancing ductility and extending the warning range before failure. The experimental results underscore the effectiveness of combining hybrid schemes with steel fibers in RC beams. The flexural capacity of the tested beams and an additional 41 specimens from the literature was determined through a modified approach based on first principles. Experimental flexural capacities were compared to theoretical ones, with an average ratio of about 1.05, indicating a reliable measure for predicting flexural capacity.

1. Introduction

Over the past few decades, there has been a notable surge in research interest focused on evaluating the efficacy of utilizing fiber-reinforced polymers (FRP) as a substitute for traditional reinforcing steel in reinforced concrete (RC) structures. This exploration stems from the potential of FRP to enhance the durability of concrete structures and address the persistent issue of steel corrosion. The challenge of steel corrosion significantly decreases the service life of structures exposed to chloride salts and poses a threat to the structural integrity of moisture-exposed structures such as dams and tanks. FRP presents several advantages, including its lightweight nature and impressive tensile strength, which can reach up to 1000 MPa. This high tensile strength allows for a substantial enhancement in the load-bearing capacity of RC sections.

Several researchers [1–4] have previously conducted comprehensive investigations, both experimental and numerical, to explore the flexural behavior of beams reinforced with FRP bars. In a particular study, ten beams, each measuring 120 mm in width, 300 mm in depth, and 2800 mm in length, were meticulously cast and subjected to testing under four-point bending [1]. The key parameters considered in this investigation included the type of reinforcement material (GFRP and steel), concrete compressive strength, and the reinforcement ratio (μb, 1.7 μb, and 2.7 μb, where μb represents the balanced reinforcement ratio). Test results revealed that an increase in the reinforcement ratio led to a significant reduction in crack widths and mid-span deflection. Moreover, the ultimate load demonstrated a substantial enhancement of 47% and 97% as the reinforcement ratio increased from μb to 2.7 μb. Particularly noteworthy was the observation that specimens reinforced with 2.7 μb exhibited a degree of ductility, which could be attributed to the concrete's behavior. The recorded strain of GFRP reinforcement reached an impressive 90% of the ultimate strains. In a separate investigation focusing on Basalt Fiber-Reinforced Polymer (BFRP) RC beams [2], the study explored the flexural behavior through a combination of numerical simulations and experimental tests. The findings highlighted two distinct failure modes for BFRP RC members. When the reinforcement ratio (μf) exceeded the balanced reinforcement ratio (μb), the beams exhibited a failure mode characterized by concrete crushing. Importantly, this type of failure was not sudden, and the beam demonstrated a measure of ductility. Conversely, when μf was lower than μb, the beams experienced a sudden failure due to reinforcement rupture.

The impact of basalt fibers on the flexural and shear behaviors of concrete beams, reinforced with BFRP bars, was experimentally assessed

* Corresponding author.
E-mail addresses: ahmed.elbakzawy@feng.bu.edu.eg (A. El Bakzawy), MOHAMED.MAKHLOUF@bhit.bu.edu.eg (M.H. Makhlouf), Tarek.mohamed@feng.bu.edu.eg (T.S. Mustafa), maher.adam@feng.bu.edu.eg (M. Adam).

https://doi.org/10.1016/j.engstruct.2024.118054
Received 2 June 2023; Received in revised form 22 March 2024; Accepted 12 April 2024

Nomenclature

SF	Steel fibers
V_f	Volume ratio of steel fibers
Ac	Area of the compression zone
a	Depth of the rectangular stress block
A_s	Area of steel reinforcement bars in tension
A_f	Area of FRP reinforcement bars in tension
ρ_f	Ratio of FRP reinforcement
ρ_s	Ratio of steel reinforcement
P_{cr}	Cracking load
P_{cr-R}	Cracking load of the reference beam
P_y	Load at yielding level
P_{y-R}	Load at the yielding level of the reference beam
δ_y	Deflection at the yielding level
δ_{y-R}	Deflection at the yielding level of the reference beam
P_u	Load at the ultimate level
P_{u-R}	Load at the ultimate level of the reference beam
δ_u	Deflection at the ultimate level
δ_{u-R}	Deflection at the ultimate level of the reference beam
K	Initial stiffness
DF	Ductility factor
HTS	High Tensile Steel
GFRP	Glass Fiber Reinforced Polymers
ε_y	Strain at the yielding level
ε_t	Strain at the ultimate level
μ_s	Strain ductility
C_c	The compression force of SFRC concrete
T_s	The tensile force in steel bars
T_f	The tensile force in GFRP bars
T_{sf}	The tensile force resulting from the steel fibers' presence in concrete
σ_{cf}	The compressive stress of SFRC
f_{cuf}	The cubic compressive strength of SFRC
f_{cu}	The cubic compressive strength of plain concrete
f'_c	The cylindrical compressive strength of plain concrete
$\frac{L_f}{\phi}$	The aspect ratio of included steel fibers
F_f	Tensile stress in GFRP bars
F_y	Yielding stress of steel bars
ε_f	Strain of FRP bars
A_{sf}	Area of the tension zone
σ_{sf}	The tensile strength resulting from steel fiber inclusion in concrete
M_n	The nominal flexural strength
M_{exp}	The experimental flexural strength

[5,6] . Twelve beams, targeting a compressive strength of 40 MPa, were cast with plain, basalt fibers, and synthetic fibers-reinforced concrete [5]. Basalt fibers of lengths 24 mm and 12 mm were considered. The test matrix included FRC beams with GFRP bars and conventional steel rebar for comparison. Results indicated improved curvature ductility and enhanced flexural capacities, attributed to delayed concrete failure strain beyond 0.003 in the compression zone, enabling BFRP bars to achieve higher ultimate strength. Addressing the limitation of ductility in RC beams when employing FRP bars is a significant concern that warrants further research. One contemporary approach to tackle this ductility challenge involves the adoption of hybrid schemes, combining FRP and steel bars. This research will explore and implement such hybrid schemes as a potential solution to enhance the ductility of RC beams.

Several researchers have investigated the enhancements in beams reinforced with FRP bars through the utilization of hybrid schemes, involving a combination of steel bars and FRP bars [7–15]. Six concrete beams were tested, reinforced with a mix of GFRP and steel bars, alongside three beams reinforced solely with steel bars [8]. Key parameters included reinforcement and area ratios of FRP to steel bars. Findings revealed that hybrid reinforced beams exhibited faster crack width and deflection development than steel-reinforced beams. Despite equal total reinforcement amounts, hybrid reinforced beams had 91–97% of the ultimate flexural capacity of steel-reinforced beams. However, deflection and crack width were notably larger in hybrid reinforced beams at equivalent service loads. The GFRP-to-steel area ratio significantly influenced their flexural behavior. In a similar context, it was observed that over-reinforced hybrid beams exhibited greater strength and ductility compared to beams reinforced solely with GFRP [11].

Experimental tests on continuous concrete beams with hybrid GFRP-steel reinforcement explored key parameters: GFRP quantity, steel reinforcements, and the steel-to-GFRP area ratio [13,14]. Findings revealed that increasing GFRP in sagging and hogging zones heightened load capacity but reduced ductility [13]. Conversely, higher steel reinforcement ratio at critical sections enhanced ductility but yielded less load capacity increase. Introducing steel to GFRP-reinforced T-beams improved flexural stiffness, ductility, and serviceability [14]. However, moment redistribution at failure was limited due to early steel yielding in sections not reaching full capacity, despite the presence of FRP reinforcement.

An alternative method of combining steel with FRP involves utilizing hybrid bars, where a steel bar serves as the core, wrapped with FRP, as demonstrated by Said et al. [16,17]. This study involved testing twelve half-scale concrete beams to investigate the flexural performance of beams reinforced with locally produced hybrid bars and hybrid schemes. The variables examined were the reinforcement bar types (hybrid, GFRP, and steel) and reinforcement ratios (0.85%, 1.26%, 1.70%, 1.8%, and 2.13%). The test results revealed a noteworthy improvement in the maximum load-carrying capacity with an increase in the hybrid reinforcement ratio. Specifically, capacities increased by 109% and 167% for hybrid reinforcement ratios of 1.26% and 1.7%, respectively. Additionally, the strain of reinforcing bars exceeded the yield level. Consequently, the use of hybrid reinforced bars or hybrid schemes exhibited increased ductility for concrete beams.

Numerous researchers have investigated the enhancement of flexural performance in RC beams by the incorporation of various types of fibers into the concrete mix [18–32]. The key parameters explored in these studies predominantly include the fiber volume (ranging from 0.25% to 2.0%), the fiber types (steel, carbon, glass, basalt, and polypropylene fibers), and the fiber shapes (hooked-end, corrugated, and plain fibers). Drawing from the outcomes of these studies, the addition of fibers to the concrete mix enhances the ductility index, inhibits crack propagation, and augments tensile strength, consequently leading to increased stiffness in the structural element. The investigation revealed that increasing the SF volume to 1.0% improved concrete tensile strength and flexural capacity by 50% [20]. Additionally, it was concluded that the yielding stress of steel reinforcement increased proportionally with the increase in SF volume ratio [26]. This led to an enhancement in the flexural capacity and ductility of the sections.

Through the examination of past studies, it is evident that the use of hybrid scheme reinforcement or SF has a substantial impact on enhancing the flexural performance and ductility of RC beams. Additionally, there is a notable improvement in the stiffness and toughness of the beams. Building on this knowledge and introducing a new approach, this research focuses on assessing the flexural performance of RC beams

a) GFRP ribbed bars (10 and 12 mm) b) Hybrid scheme (steel and GFRP bars)

Fig. 1. Produced GFRP and steel bars.

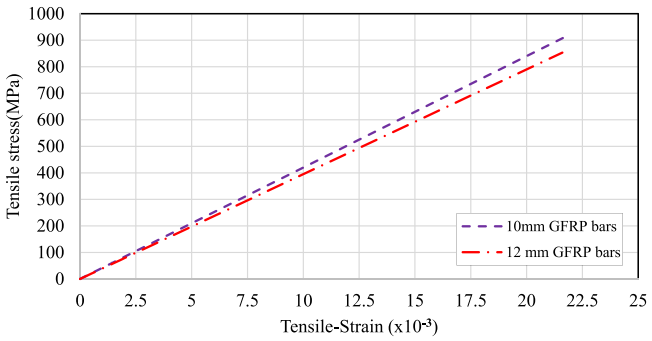

Fig. 2. Stress-strain curve of GFRP bars.

incorporating both hybrid longitudinal reinforcements and steel fibers. Seven half-scale SFRC beams, reinforced with hybrid schemes, underwent experimental testing to quantify improvements in various aspects, including load capacity, ductility, toughness, and flexural capacity of the RC beams.

2. Test program

2.1. Material properties

2.1.1. Manufacturing and testing of GFRP bars

GFRP ribbed bars were locally manufactured by the author, using resin and glass fiber roving. Plastic molds were made in a special workshop for manufacturing with length of 12 m and diameters of 10 and 12 mm as shown in Fig. 1.

Specimens from the GFRP bars were experimentally tested to determine their tensile strength and mechanical properties. The average tensile strength of GFRP bars with 10 mm and 12 mm diameters was respectively 910 MPa and 850 MPa with modulus of elasticity 42 GPa and 39 GPa. The outer surface of GFRP bars was deformed to enhance the bond between the bars and the concrete. The stress-strain curve of the tested GFRP bars is illustrated in Fig. 2.

2.1.2. Steel bars

Longitudinal reinforcement consisted of deformed steel bars with a yield strength of 400 MPa. Stirrups for all beams were made from normal mild steel bars, 8 mm in diameter, with a nominal yield strength of 240 MPa. Additionally, all steel bars used in the study shared an elasticity modulus of 200 GPa. Both steel and GFRP bars with close spacing adhere to the principles outlined in relevant codes and standards, which permit the use of bundled reinforcement configurations. This concept has been investigated by Suna et al. [33] and is documented across various design code standards.

2.1.3. Steel fibers

The used fiber in the FRC (Fiber Reinforced Concrete) was corrugated steel fiber with a tensile strength of 1000 MPa and elastic modulus of 200 GPa. The length and diameter of the steel fibers were respectively 50 mm and 1.0 mm with a length/diameter ratio of 50.

2.1.4. Concrete mixtures

The concrete mixes were made using high-quality components. Among them was naturally occurring, pure siliceous sand that was devoid of contaminants like silt, clay, or loam. The specific gravity of the sand was 2.6 and its fineness modulus was 2.65. A maximum aggregate size of 16 mm of crushed dolomite with a specific gravity of 2.5 and a fineness modulus of 4.3 was used. Furthermore, ordinary Portland cement and freshwater were used in the mixture. The coarse aggregate underwent a washing process to eliminate fines and dirt prior to mixing. Subsequently, sand and coarse aggregate were combined in their dry state, followed by the addition of cement. Mixing persisted for 2 min until a uniform color was observed. Gradually, water was introduced to the dry components in a rotary machine. To ensure thorough homogenization among the constituents, the concrete underwent mixing for nearly 4 min. Steel fibers are added to the concrete mix during the mixing process after the aggregates and cement have been thoroughly combined. This ensures proper dispersion of the fibers throughout the concrete mixture, allowing them to enhance the mechanical properties of the resulting material effectively.

The slump test for concrete is a crucial aspect of assessing its workability and consistency. During the slump test, a conical mold is filled with freshly mixed SFRC in layers, each compacted using a specified rod. After filling, the mold is lifted vertically, allowing the concrete to spread and settle. The difference in height between the original and final position of the concrete is measured, indicating the slump value. In SFRC, the addition of steel fibers can influence the slump behavior. Generally, SFRC tends to exhibit lower slumps compared to conventional concrete due to the fibers' presence, which impedes the flow of the mixture.

Table 1
Test results for compressive strength, tensile strength, and slump.

Ingredient	Cement (Kg/m^3)	Fine aggregate (Kg/m^3)	Coarse aggregate (Kg/m^3)	Water (Kg/m^3)	Average Compressive Strength (MPa)	Average splitting tensile strength (MPa)	Slump mm
SFRC 0%	350	680	1400	175	30.00	3.20	70
SFRC 1%	350	680	1400	175	30.30	3.80	60
SFRC 2%	350	680	1400	175	31.00	4.45	50

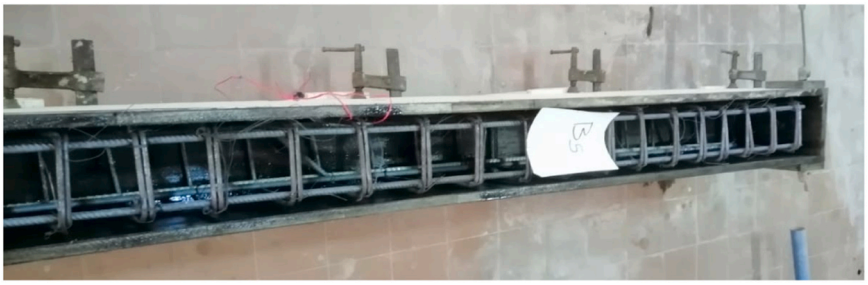

Fig. 3. Wooden form and reinforcement details of the test beams.

However, the slump value can vary depending on factors such as fiber type, length, and content, as well as mix proportions and workability-enhancing admixtures. The slump tests conducted on the fresh concrete specimens indicated a decrease in slump as the steel fiber content increased. This phenomenon can be attributed to the presence of steel fibers, which tend to impede the flow of the mixture. The recorded slump values for the concrete mixes containing steel fibers at levels of 0.0%, 0.5%, and 1.0% are 70 mm, 60 mm, and 50 mm, respectively. The results of the slump test revealed that the degree of workability is medium, which could be reasonable for casting normal reinforced concrete placed with vibration.

The test results of the concrete are illustrated in Table 1. The compressive strength, tensile strength, and slump tests result provided encompass both normal concrete and SFRC associated with the properties of each mix.

2.2. Test specimens

Seven concrete beams reinforced with reinforcing steel or hybrid schemes and containing steel fibers were designed as a simply supported span with an adequate amount of longitudinal and shear reinforcement. The study addressed the effect of main parameters on the flexural behavior of concrete beams (ductility, cracking load, ultimate capacity load, and deflection). The Main parameters were the steel fiber volume ratio (V_f) and the ratio between steel and GFRP reinforcement in the hybrid schemes. The form and reinforcement details of the test beams are shown in Fig. 3.

The beam specimens were divided into three groups (A, B, and C). Each group consists of beams with different SF volume ratios (0.00%, 0.50%, and 1.00%). Two different reinforcement ratios (0.94% and 1.14%) were used. The reinforcement used in all specimens was a hybrid scheme except for specimen B1 the reinforcement used was steel bars only. The geometry and parameters of the tested beams are illustrated in Fig. 4 and Table 2.

2.3. Test setup

The beams were tested at a hydraulic machine with a 1000 kN capacity. A rigid steel beam divided the load into two points separated by 400 mm. The two loads were symmetric about the center of the beam. A linear variable differential transformer (LVDT) was installed at the midpoint of beams to record the mid-span deflection of each 1.0 kN increment. The typical test setup for the beam specimens is illustrated in Fig. 5.

3. Experimental results and discussion

3.1. Cracking and ultimate loads

The cracking load was recorded for all beams by well observation of the beam until the appearance of the first crack and recording the corresponding load. The ultimate load for each beam was also recorded. Table 3 summarizes the observed test results for Group A, Group B, and Group C respectively. The results showed that there is a significant enhancement in the first crack load and the ultimate load by increasing the steel fiber ratio in the beam. Also, the ultimate load increases by increasing the GFRP reinforcement ratio in the longitudinal reinforcement.

In Group A, no improvement in the first crack load was observed when employing hybrid schemes with the same reinforcement ratio or increasing the ratio of GFRP in the longitudinal reinforcement in beams B2 or B3, compared with B1. However, the ultimate load increased by 8% in B2 when using hybrid schemes with the same reinforcement ratio and by 14% in B3 when increasing the GFRP ratio from 0.47% to 0.67%. It is evident that the enhancement in the maximum load is not significant when employing the same tension reinforcement ratio for the hybrid scheme instead of steel. This is attributed to the low ductility of the beam, as the strain of the GFRP bars increases significantly after the steel bars yield, leading to the rapid failure of beams. For Group B, consisting of specimens B4 and B5, the use of 0.50% steel fiber volume increased the first crack load by 12.5% more than specimens B2 and B3 in Group A. Moreover, the enhancement in the maximum load was 12% and 13% for B4 and B5, respectively. In Group C, comprising specimens B6 and B7, where the steel fiber ratio was increased to 1.00%, the cracking load improved by 19% and 25% compared to the test results with specimens B2 and B3, respectively. Additionally, the load-carrying capacity increased by 21% for both specimens B6 and B7.

Analyzing the findings from prior research studies reveals an 11% improvement in load-carrying capacity when comparing hybrid scheme-reinforced beams with FRP-reinforced beams [14]. Exploring hybrid schemes as bundled bars in [15], where longitudinal reinforcement included steel and FRP bundles, led to a 4.5% increase in cracking load and a 5.6% increase in ultimate load. Conversely, employing hybrid bundles (steel bar & FRP bar) resulted in a 5.5% decrease in cracking load but a notable 10.3% increase in ultimate load. The inclusion of steel fibers in [18] enhanced the cracking load by varying ratios based on the depth of the steel fiber-reinforced part in the beam, with a maximum enhancement ratio of 92% for fully reinforced sections. Additionally, the maximum load exhibited a slight increase depending on the depth of the steel fiber-reinforced part, significantly improving in fully steel fiber-reinforced beams with a 22% enhancement ratio. This underscores the effectiveness of uniformly incorporating steel fibers across the depth in delaying crack formation and increasing the flexural capacity.

The observed improvement in the first crack load occurs due to the role of the steel fibers in the tension zone in resisting crack propagation and decreasing the crack width. Also, the maximum load was improved by increasing the steel fiber ratio because of increasing the concrete ductility due to the presence of the steel fibers in the compression zone leading to a higher level of warnings before failure. Therefore, it can be concluded that the addition of steel fibers to beams reinforced with hybrid schemes significantly improves the cracking load and ultimate load.

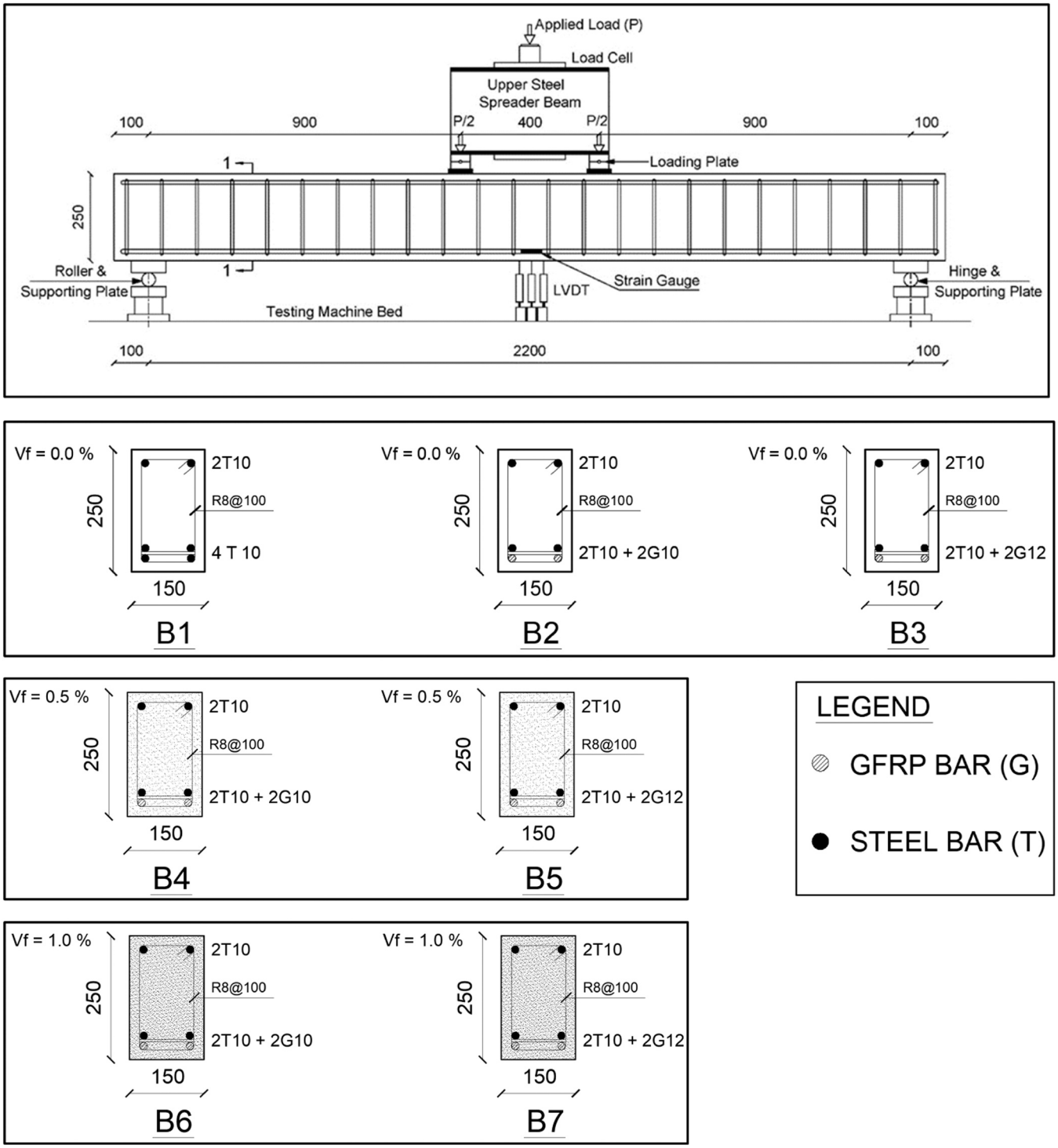

Fig. 4. Geometry and details of the tested beams.

3.2. Load-deflection curves

The experimental load-deflection curves for Groups A, B, and C are illustrated in Fig. 6. Load-deflection curves typically exhibit three primary stages. The initial stage is characterized by linear behavior, representing the response until the occurrence of the first crack. The second stage reflects the response until the yielding of the steel reinforcement. The third and final stage is marked by a significant increase in deflection with successive loads until failure. In Group A, the deflection before failure for B2 and B3 was observed to be less than that of B1. However, the failure load for B2 and B3 is more than that of B1, indicating that specimens B2 and B3 are less ductile than B1. These experimental results confirm that the use of GFRP in hybrid schemes decreases the ductility of the beams.

In Group B, steel fiber was introduced to the concrete mix with a 0.50% volume ratio. The deflection before failure in specimens B4 and B5 was significantly larger than that of B1, and the ultimate load also showed a substantial increase. In Group C, where the steel fiber volume ratio was further increased to 1.00%, the deflection before failure in specimens B6 and B7 markedly increased, although the ultimate load

Table 2
Details of the tested beams.

Group	Beam	V_f	Bottom reinforcement		Bottom reinforcement ratio			Stirrups	Top reinforcement
			Af	As	ρ_f	ρ_s	ρ_t		
A	B1	0.0%	—	4T10	0.00%	0.94%	0.94%	ϕ8 / 100	2T10
	B2	0.0%	2G10	2T10	0.47%	0.47%	0.94%	ϕ8 / 100	2T10
	B3	0.0%	2G12	2T10	0.67%	0.47%	1.14%	ϕ8 / 100	2T10
B	B4	0.5%	2G10	2T10	0.47%	0.47%	0.94%	ϕ8 / 100	2T10
	B5	0.5%	2G12	2T10	0.67%	0.47%	1.14%	ϕ8 / 100	2T10
C	B6	1.0%	2G10	2T10	0.47%	0.47%	0.94%	ϕ8 / 100	2T10
	B7	1.0%	2G12	2T10	0.67%	0.47%	1.14%	ϕ8 / 100	2T10

Fig. 5. Typical test setup for the beam specimens.

improvement was not significantly improved. These experimental findings prove and highlight the efficiency of steel fiber addition in enhancing the ductility of concrete beams reinforced with hybrid schemes.

Based on the recorded experimental load-deflection curves in Fig. 6, the following measurements can be evaluated as follows:

3.2.1. Initial stiffness (K)

Stiffness is defined as the ratio between the load at the yield point (P_y) to the corresponding displacement (δ_y) [16]. Fig. 7 illustrates the experimental results of stiffness for the tested beams. In Group A, compared with control specimen B1, the stiffness of the specimens B2 and B3 was reduced by 27% and 25% respectively. As a result, the stiffness of the beam decreases by using GFRP bars in hybrid schemes instead of steel bars. In Group B, the stiffness of B4 and B5 showed enhancement by 17% and 4% respectively compared with B2 and B3 in Group A (including the same longitudinal reinforcement without the addition of steel fiber to the concrete mix). In Group C, it was observed that the stiffness of beams B6 and B7 increased by 21% and 25% respectively compared with beams B2 and B3 in Group A. These findings align with the outcomes presented in [14], which observed a reduction in mid-span deflection of beams by varying proportions when employing hybrid schemes instead of GFRP bars. The stiffness enhancement ratio exhibited an increase with the higher ratio of steel bars in hybrid schemes, reaching a maximum enhancement ratio of 14%. Additionally, the utilization of bundled hybrid schemes, as reported in [15], resulted in an initial stiffness increase of 1.6% in beams.

The experimental findings validate the significant contribution of steel fibers in enhancing the stiffness that had been diminished due to the incorporation of GFRP in hybrid schemes. Moreover, as the steel fiber volume ratio increases from 0.50% to 1.00%, the ratio of stiffness enhancement also experiences an increase. This enhancement is attributed to the steel fibers' resistance to crack propagation and the concurrent reduction in crack width. These factors collectively enhance the effective moment of inertia I_{eff} of the section, leading to reduced deflection and consequently higher stiffness.

3.2.2. Energy absorption (Toughness)

Toughness is defined as the area under the load-deflection curve as a function of the ultimate load (P_u) and the corresponding deflection (δ_u). Accordingly, toughness is a good measure of the ductility of the beam. Fig. 8 illustrates the experimental results of toughness for the tested beams. In Group A, compared with B1, the toughness of B2 and B3 was reduced by 7.0% and 12.7% respectively. In Group B, compared with B2 and B3 in Group A, the toughness of beams B4 and B5 was improved by 97.7% and 71% respectively. In Group C, the toughness of B6 and B7 increased by 139.4% and 105% respectively when compared with B2 and B3 in Group A. It can be concluded that the addition of steel fibers to the concrete mix in the hybrid reinforced beams significantly enhances the toughness. Additionally, the enhancement of the toughness increases by increasing the steel fiber volume from 0.50% to 1.00%. Similar outcomes were documented in [14], where the adoption of hybrid

Table 3
Experimental results of the tested beams.

Group	Beam	V_f (%)	Experimental Test Results							Relative Exp. Results to the Control Beam						
			P_{cr} (kN)	P_y (kN)	δ_y (mm)	P_u (kN)	δ_u (mm)	K (kN /mm)	DF	$\frac{P_{cr}}{P_{cr-R}}$	$\frac{P_y}{P_{y-R}}$	$\frac{\delta_y}{\delta_{y-R}}$	$\frac{P_u}{P_{u-R}}$	$\frac{\delta_u}{\delta_{u-R}}$	$\frac{K}{K_R}$	$\frac{DF}{DF_R}$
A	B1	0.00	17.00	75.50	12.14	82.20	60.75	6.21	5.00	1.00	1.00	1.00	1.00	1.00	1.00	1.00
	B2	0.00	16.00	55.20	12.12	89.00	59.60	4.55	4.91	0.94	0.73	0.99	1.08	0.98	0.73	0.98
	B3	0.00	16.00	58.10	12.60	94.00	52.97	4.62	4.20	0.94	0.77	1.04	1.14	0.87	0.75	0.84
B	B4	0.50	18.00	52.20	9.78	100.20	97.44	5.33	9.96	1.12	0.94	0.81	1.12	1.63	1.17	2.03
	B5	0.50	18.00	55.10	11.47	105.90	79.72	4.81	6.95	1.12	0.95	0.91	1.13	1.51	1.04	1.65
C	B6	1.00	19.00	55.30	10.00	108.10	116.80	5.53	11.7	1.19	1.00	0.82	1.21	1.95	1.21	2.38
	B7	1.00	20.00	55.90	9.68	114.20	94.57	5.77	9.76	1.25	0.96	0.77	1.21	1.78	1.25	2.32

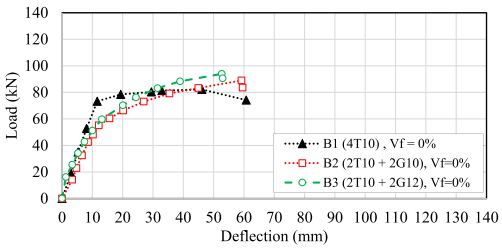

(a) Effect of the steel/GFRP ratio in the hybrid schemes on the load-deflection curves

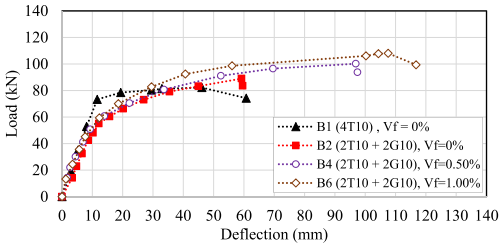

(b) Effect of SF volume on the load-deflection curves for beams reinforced by hybrid schemes

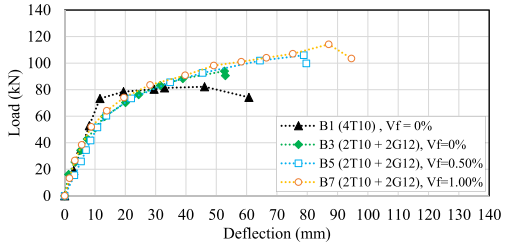

(c) Effect of SF volume on the load-deflection curves for beams reinforced by hybrid schemes

Fig. 6. Load-deflection curves of the tested beams.

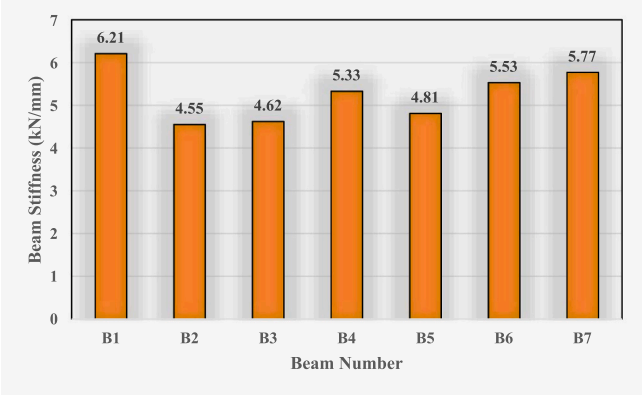

Fig. 7. Experimental stiffness of the tested beams.

schemes in lieu of GFRP bars led to a 19% increase in the toughness of beams for an equivalent area of longitudinal reinforcement.

3.2.3. *Ductility factor*

The ductility factor is defined as the ratio between the deflection at the failure point (δ_u) to the deflection at the yield point (δ_y). The yield point deflection (δ_y) for ductility calculation can be identified as the displacement at which the load-deflection curve begins to exhibit a notable bend or deviation from its original behavior. This deviation indicates the initiation of plastic deformation, marking the onset of yielding and the transition to nonlinear behavior. Fig. 9 presents the experimental results of ductility for the tested beams. Incorporating steel fibers into the concrete mixture notably heightened the ductility factor, which decreased when utilizing hybrid schemes that included GFRP bars. In Group A, the ductility factor exhibited a degradation of 2% and

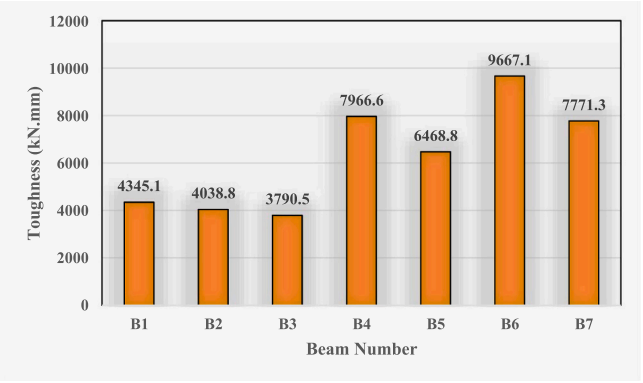

Fig. 8. Experimental toughness of the tested beams.

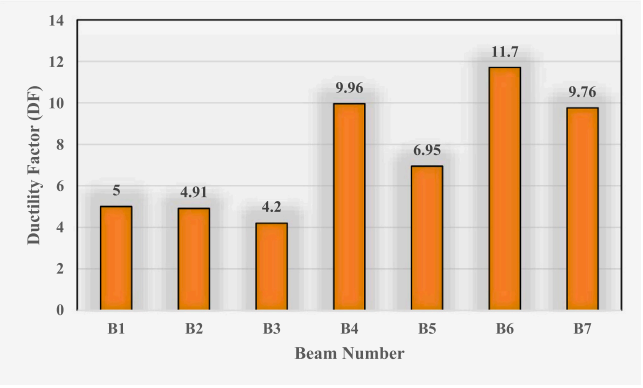

Fig. 9. Experimental ductility of the tested beams.

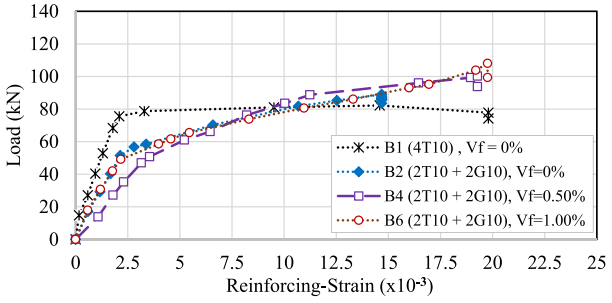

(a) Load- reinforcing strain of the tested beams (B1, B2, B4, and B6)

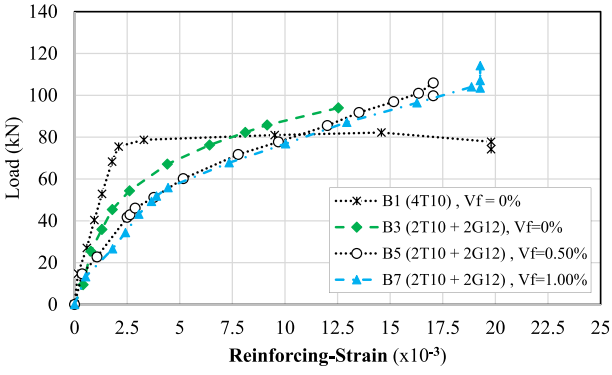

(b) Load- reinforcing strain of the tested beams (B1, B3, B5, and B7) (Cont.)

Fig. 10. Load- reinforcing strain of the tested beams.

Table 4
Tensile strains of the steel and GFRP bars at the yield level and ultimate levels.

	Beam	Type of Bar	Reinforcing Strain at Yield level, (εy)	Reinforcing Strain at Ultimate level, (εt)	Strain Ductility, $\mu s = \frac{\varepsilon t}{\varepsilon y}$	Mode of failure
A	B1	HTS	0.0020	0.0197	9.85	Steel yielding.
	B2	HTS GFRP	0.0020 0.0028	0.0218 0.0146	10.90 5.21	Steel yielding, concrete crushing
	B3	HTS GFRP	0.0020 0.0031	0.0218 0.0125	10.90 4.03	Steel yielding, concrete crushing
B	B4	HTS GFRP	0.0020 0.0032	0.0215 0.0180	10.75 5.62	Steel yielding, concrete crushing
	B5	HTS GFRP	0.0020 0.0037	0.0215 0.0170	10.75 4.59	Steel yielding, concrete crushing
C	B6	HTS GFRP	0.0020 0.0031	0.0215 0.01 97	10.75 6.35	Steel yielding, concrete crushing
	B7	HTS GFRP	0.0020 0.0039	0.0192 0.0192	9.60 4.92	Steel yielding, concrete crushing

16%, respectively, when compared to specimen B1. In Group B, the ductility factor for B4 and B5 improved by 103% and 65%, respectively, in comparison to beams B2 and B3 in Group A. In Group C, the ductility factor for B6 and B7 increased by 138% and 132%, respectively, compared to beams B2 and B3 in Group A. The experimental results affirm that the flexural performance of concrete beams reinforced with hybrid schemes showed significant improvement through the addition of steel fibers to the concrete mix. Notably, the ductility factor experienced a decrease of 23% when employing bundles of hybrid schemes (combining steel bars and GFRP bars), attributed to the concentration of tension stresses. Comparing ductility results with the previous studies indicates that introducing steel fiber to specific zones decreased the ductility factor by a maximum of 31.5% [18], while fully steel fiber-reinforced beams reached a 7.5% increase. Adding polyvinyl alcohol fibers to hybrid scheme-reinforced beams enhanced the ductility factor by 20% and 27% for fiber volume ratios of 0.75% and 1.5%, respectively [17].

3.3. Strains in steel and GFRP bars

Strain gauges were fixed to measure the strains in the tension longitudinal reinforcement of the test beams as shown in Fig. 4. The gauges were fixed in the middle of the bars. The load-reinforcing strain curves for all beams are shown in Fig. 10. The strains of steel bars and GFRP bars at the yield level and ultimate level are presented in Table 4.

Analyzing the strains of the tension reinforcement bars, it was observed that the strains in the tension steel bars for all beams at the ultimate level exceeded the yield strain (ε_y), indicating that yielding of the steel bars occurred before the failure of the beams. The measured strains of GFRP bars at the ultimate level were 0.0146, 0.0125, 0.018, 0.017, 0.0197, and 0.0192 for beams B2, B3, B4, B5, B6, and B7, respectively. Notably, these strain values are less than the ultimate strain of GFRP bars (0.022). Consequently, the rupture of GFRP bars did not occur at the beams' failure. Instead, the beams failed in a ductile manner, characterized by steel bars yielding, followed by concrete crushing, and ultimately, GFRP bars rupture. This mode of failure is preferable as it provides substantial warning, especially after enhancing the toughness of beams by incorporating steel fiber to the concrete mix.

(a) Crack Patterns for the Tested Beam B1

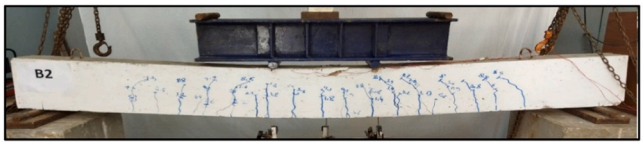

(b) Crack Patterns for the Tested Beam B2

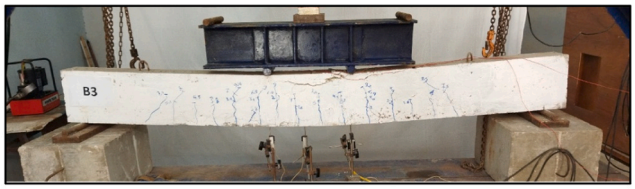

(c) Crack Patterns for the Tested Beam B3

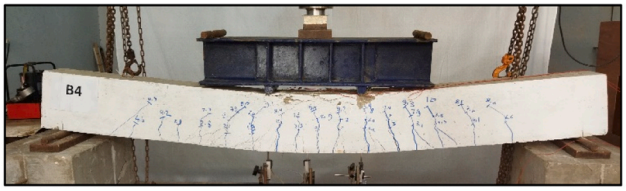

(d) Crack Patterns for the Tested Beam B4

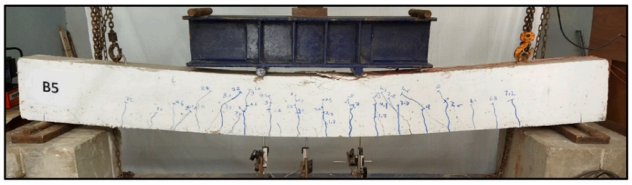

(e) Crack Patterns for the Tested Beam B5

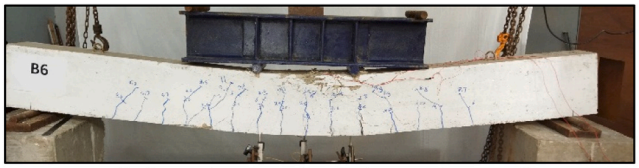

(f) Crack Patterns for the Tested Beam B6

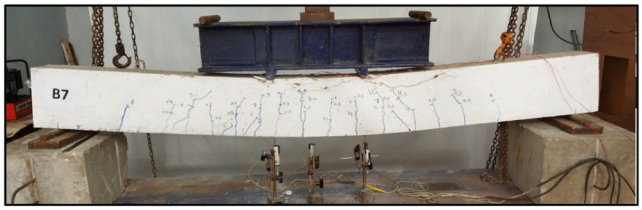

(g) Crack Patterns for the Tested Beam B7

Fig. 11. Crack Patterns for the Tested Beams.

In Group A, it was observed that the strain values for GFRP bars at the ultimate level in beams B2 and B3 were relatively small. Consequently, the failure occurred rapidly due to concrete crushing with a low level of warnings. In contrast, for Group B and Group C, the strain values of GFRP bars at the ultimate level for beams B4, B5, B6, and B7 were relatively large and closer to the ultimate strain value. The experimental results elucidate that the failure occurred with a higher level of ductility

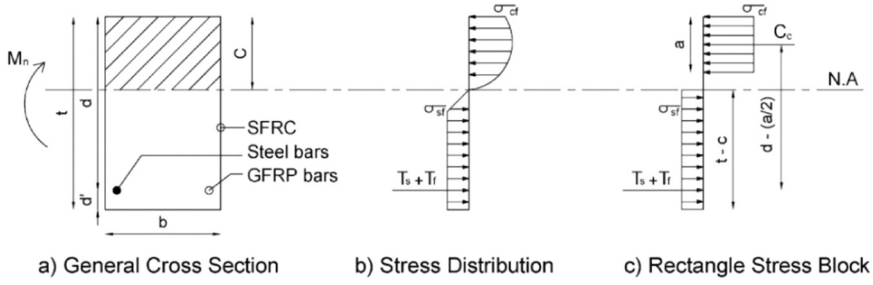

Fig. 12. The stress distribution along the cross-section of SFRC Beams.

and warnings, attributed to the improved energy absorption of concrete resulting from the addition of steel fibers to the concrete mix. This enhancement amplifies the advantages derived from the presence of GFRP bars in the longitudinal reinforcement of the beams.

The values of strain ductility (μs) were assessed from the load-strain curves, defined as the ratio between strains in the reinforcing bars at the ultimate level to the strains at the yield level. The experimental results affirm that adding steel fiber plays a crucial role in enhancing the value of (εt), leading to improved strain ductility. Moreover, the enhancement ratio increases with an increase in the steel fiber volume ratio. These experimental results shed light on the significance of employing hybrid schemes of reinforcement, especially in the presence of steel fibers, as a modern and effective technique.

3.4. Failure modes and cracks pattern

One crucial method for determining failure modes and understanding the failure process is tracking crack paths and noting the associated loads at various loading levels. This approach is essential for studying the influence of parameters on the performance of the tested beams. The crack patterns of the tested beams are illustrated in Fig. 11. At first, initial cracks appeared at the mid-span of all beams in the maximum moment region. Subsequently, as the load increments increased, the cracks propagated away from the middle of the beams and approached the supports. The width and depth of cracks in the maximum moment area expanded with escalating load values until reaching the failure level. The failure mechanism observed in the tested beams was flexural failure, characterized by the yielding of steel bars followed by concrete crushing before the rupture of GFRP bars.

For Group A, using hybrid schemes in beams B2 and B3 accelerated the appearance of the first crack compared with the beam B1 reinforced by steel bars only. At the failure level, the using of hybrid schemes led to increasing the propagation and width of the visual cracks. In Group B, the utilization of steel fibers with a 0.50% volume ratio in B4 and B5 postponed the onset of the first crack compared to beams without steel fibers in Group A. This resulted in increased ductility and energy absorption of the beams, along with the development of stapling cracks and a reduction in their propagation. Consequently, this enhanced the load capacity of the beams, preventing the occurrence of sudden brittle failure of the beams. In Group C, increasing the steel fiber volume ratio from 0.50% to 1.00% delayed the onset of the first crack while simultaneously improving the ductility and toughness of the beams. This enhancement contributes to increased load capacity, mitigating the risk of sudden brittle failure.

4. Nominal flexural capacity

A modified approach based on first principles [34] was employed to predict the nominal flexural capacity of SFRC beams reinforced with hybrid schemes. The novelty of this approach lies in the calculation of the nominal flexural strength, which considers the tension forces arising from both the steel and GFRP bars of the hybrid reinforcement, as well as the randomly distributed steel fibers in the tension zone. Additionally, this approach is applicable to both hybrid reinforced SFRC beams and steel reinforced SFRC beams. This method was applied to predict the nominal flexural capacity of 48 beams, including those tested in this research and 41 beam specimens from the literature. The calculated experimental moments for all 48 beams were compared with the predicted nominal flexural moments, considering the presence of GFRP bars and steel fibers with varying volume ratios in all beam sections. Fig. 12 illustrates the stress blocks used in calculating the tensile forces in steel bars, GFRP bars, steel fibers, and the compressive force resulting from SFRC on the compression side. The equilibrium equation can be expressed as follows:

$$C_c = T_s + T_f + T_{sf} \tag{1}$$

Where C_c represents the compression force of SFRC, and it can vary depending on the steel fiber volume ratio and the rectangular stress block, as follows:

$$C_c = \sigma_{cf} * A_c \tag{2}$$

The compressive stress of SFRC, σ_{cf} can be defined as follows [26]:

$$\sigma_{cf} = 0.67 * f_{cuf} \tag{3}$$

The cubic compressive strength of SFRC (f_{cuf}) can be defined [26] as:

$$f_{cuf} = f_{cu} * (1 + 0.1066 * V_f * \frac{L_f}{\phi}) \tag{4}$$

Where f_{cu} is the cubic compressive strength of concrete.

V_f represents the volume ratio of steel fibers.

$\frac{L_f}{\phi}$ represents the aspect ratio of steel fibers.

The area of the compression zone is defined as: $A_c = a * b$(5).

The depth of the compressive zone (a) is defined as: $a = \beta_1 * C$(6).

The factor β_1 shouldn't exceed 0.85 and should be no less than 0.65. It can be calculated as follow:

$$\beta_1 = 1.05 - 0.05 * (\frac{f_{cuf}}{6.9}) \tag{7}$$

Therefore, the compressive force C_c can be defined as:

$$C_c = 0.67 * f_{cu} * \left(1 + 0.1066 * V_f * \frac{L_f}{\phi}\right) * b * a \tag{8}$$

The tension force in reinforcing steel and GFRP bars can be defined as follows:

$$T_s = A_s * F_s \tag{9}$$

$$T_f = A_f * F_f \tag{10}$$

The tensile force in steel bars can be calculated from Eq. (9), where $F_s = F_y$ in the case of steel bars yielding before failure, which occurred in all tested beams.

The tensile force in GFRP bars can be calculated from Eq. (10), and the tensile stress in GFRP bars (F_f) can be calculated as $F_f = \varepsilon_f * E_f$ where E_f is the elasticity modulus of GFRP bars and ε_f represents the nominal

Table 5
Experimental and nominal flexural capacities of the tested beams and 41 beams from literature.

Reference	*Beam*	f_{cu}	*Geometrical Parameters*				*Bottom RFT*						*S.F Parameters*			*Experimental moment, M_{exp}*	*Nominal moment, M_n*	$\frac{M_{exp}}{M_n}$
		MPa	*b (mm)*	*d (mm)*	L_{cl-cl} *(mm)*	*X (mm)*	A_s *HTS*	F_y *MPa*	A_f *FRP*	F_f *MPa*	A_{hr} *HRB*	ρ_t *%*	V_f *%*	L_f *(mm)*	ϕ_f *(mm)*	*(kN.m)*	*(kN.m)*	
Present	B1	30	150	225	2100	800	4ϕ10	463	—	—	—	0.93	0.00	50	1	30.20	29.2	1.03
	B2	30	150	225	2100	800	2ϕ10	463	2G10	1035	—	0.93	0.00	50	1	35.60	35.15	1.01
	B3	30	150	225	2100	800	2ϕ10	463	2G12	960	—	1.13	0.00	50	1	37.60	37.67	1.00
	B4	30	150	225	2100	800	2ϕ10	463	2G10	1035	—	0.93	0.50	50	1	40.10	40.66	0.98
	B5	30	150	225	2100	800	2ϕ10	463	2G12	960	—	1.13	0.50	50	1	42.36	44.16	0.96
	B6	30	150	225	2100	800	2ϕ10	463	2G10	1035	—	0.93	1.00	50	1	43.25	42.69	1.01
	B7	30	150	225	2100	800	2ϕ10	463	2G12	960	—	1.13	1.00	50	1	45.68	47.40	0.96
Dong,et al.	S16	32.5	200	357	3600	1500	2ϕ16	449	—	—	—	0.56	—	—	—	—	74.7	—
[4]	G12-N	32.5	200	359	3600	1500	—	—	2G12	947	—	0.32	—	—	—	72.80	91.7	1.26
	G12-P	32.5	200	347	3600	1500	—	—	2G12	947	—	0.33	—	—	—	74.60	98.3	1.32
	G12-W	32.5	200	347	3600	1500	—	—	2G12	947	—	0.33	—	—	—	74.20	98.4	1.33
	G16-N	32.5	200	357	3600	1500	—	—	2G16	889	—	0.56	—	—	—	100.20	124.6	1.24
	G16-P	32.5	200	347	3600	1500	—	—	2G16	889	—	0.58	—	—	—	101.50	108.8	1.07
	C12-N	32.5	200	359	3600	1500	—	—	2C12	1890	—	0.32	—	—	—	118.60	123.6	1.04
	C12-P	32.5	200	347	3600	1500	—	—	2C12	1890	—	0.33	—	—	—	119.80	142.0	1.19
	C16-N	32.5	200	357	3600	1500	—	—	2C16	1600	—	0.56	—	—	—	146.20	158.9	1.09
	C16-P	32.5	200	347	3600	1500	—	—	2C16	1600	—	0.58	—	—	—	140.90	156.0	1.11
El Refai, et al.	B1	40	230	275	3700	1250	—	—	2G12	1000	—	0.38	—	—	—	49.03	50.28	0.97
[11]	B2	40	230	275	3700	1250	—	—	3G12	1000	—	0.64	—	—	—	53.78	51.42	1.05
	B3	40	230	275	3700	1250	—	—	3G16	1000	—	1.12	—	—	—	69.55	67.31	1.03
	B4	40	230	275	3700	1250	1ϕ10	520	2G12	1000	—	0.51	—	—	—	47.62	47.27	1.00
	B5	40	230	275	3700	1250	2ϕ10	520	2G12	1000	—	0.55	—	—	—	53.55	58.43	0.92
	B6	40	230	275	3700	1250	2ϕ12	520	2G12	1000	—	0.67	—	—	—	58.94	55.72	1.06
	B7	40	230	275	3700	1250	2ϕ10	520	2G16	1000	—	0.85	—	—	—	68.30	71.41	0.96
	B8	40	230	275	3700	1250	2ϕ12	520	2G16	1000	—	0.96	—	—	—	64.71	70.92	0.91
	B9	40	230	275	3700	1250	2ϕ16	520	2G16	1000	—	1.13	—	—	—	83.53	81.39	1.03
Araba, et al.	C-S-1	50.5	200	275	2600	1300	3ϕ16	580	—	—	—	1.10	—	—	—	97.30	85.0	1.14
[13]	C-G-1	48.0	200	275	2600	1300	—	—	2G12.7	1200	—	0.51	—	—	—	65.60	61.0	1.08
	C-H-1	50.7	200	275	2600	1300	2ϕ16	580	2G12.7	1200	—	1.24	—	—	—	92.00	88.0	1.04
	C-H-2	54.0	200	275	2600	1300	3ϕ16	580	2G12.7	1200	—	1.60	—	—	—	112.00	105.0	1.06
	C-H-3	54.6	200	275	2600	1300	2ϕ25	580	2G12.7	1200	—	2.29	—	—	—	125.00	128.0	0.98
	C-H-4	70.6	200	275	2600	1300	2ϕ16	580	3G15.9	1200	—	1.93	—	—	—	128.00	143.0	0.90
	C-H-5	75.0	200	275	2600	1300	2ϕ16	580	5G15.9	1200	—	2.73	—	—	—	160.00	169.0	0.95
	S-G-1	72.0	200	275	2600	1300	—	—	2G12.7	1200	—	0.51	—	—	—	77.00	70.0	1.10
	S-H-1	63.2	200	275	2600	1300	2ϕ8	580	2G9.5	1100	—	0.49	—	—	—	62.00	61.9	1.00
	S-H-2	66.6	200	275	2600	1300	2ϕ16	580	2G12.7	1200	—	1.24	—	—	—	110.00	99.0	1.10
M. Said, et al.	B1	45	150	275	2100	850	3ϕ12		—	—	—	0.85	—	—	—	39.1	36.75	1.06
[16]	B2	45	150	275	2100	850	—	—	—	—	2H14	0.85	—	—	—	66.73	60.35	1.11
	B3	45	150	275	2100	850	—	—	—	—	3H14	1.26	—	—	—	81.73	82.45	0.99
	B4	45	150	275	2100	850	—	—	—	—	4H14	1.70	—	—	—	104.55	102.85	1.02
	B5	45	150	275	2100	850	—	—	—	—	5H14	2.13	—	—	—	118.58	120.28	0.98
	B6	45	150	275	2100	850	4ϕ12 + 1ϕ10	400	—	—	—	1.26	—	—	—	64.64	58.65	1.10
	B7	45	150	275	2100	850	2ϕ10	400	—	—	2H14	1.26	—	—	—	79.48	73.10	1.09
	B8	45	150	275	2100	850	2ϕ10	400	3G12	850	—	1.26	—	—	—	72.68	69.70	1.04
	B9	45	150	275	2100	850	—	—	2G12	850	2H14	1.27	—	—	—	86.28	84.15	1.02
	B10	45	150	275	2100	850	—	—	3G12	850	1H14	1.27	—	—	—	84.78	81.13	1.04
	B11	45	150	275	2100	850	—	—	3G12	850	2H14	1.70	—	—	—	103.95	102.43	1.01
	B12	45	150	275	2100	850	—	—	4G12	850	2H14	1.80	—	—	—	108.38	111.35	0.97
Number of Specimens																		48
Average																		1.05
Standard deviation																		0.093

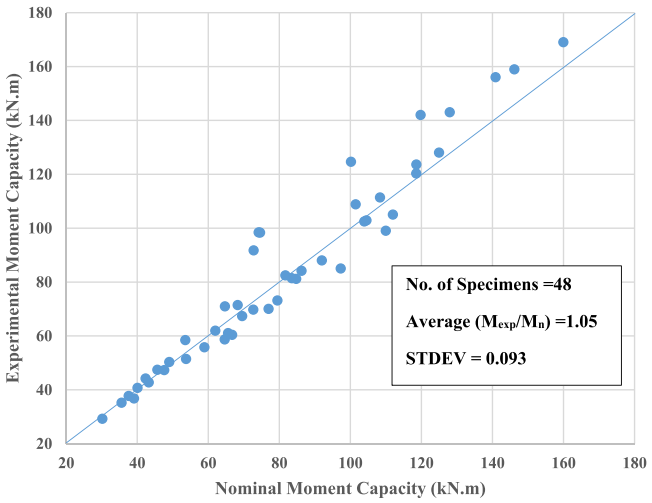

Fig. 13. comparative analysis between the experimental and nominal flexural capacities of 48 beams, incorporating those tested in this research.

strain of GFRP bars at the failure level [35], which can be determined by the following calculation:

$$\frac{c}{d} = \frac{\varepsilon_{cu}}{\varepsilon_{cu} + \varepsilon_f} \tag{11}$$

where c is the depth from the top fiber to the neutral axis, d is the effective depth, and ε_{cu} is the ultimate strain of concrete and shall be taken as 0.003.

The tensile force resulting from the inclusion of steel fibers in concrete can be calculated as follows:

$$T_{sf} = \sigma_{sf} * A_{sf} \tag{12}$$

The area of the tension zone (A_{sf}) can be calculated as: $A_{sf} = b * (t - c) = b * (t - \frac{a}{\beta 1})$ (13).

The tensile strength resulting from the inclusion of steel fiber in concrete (σ_{sf}) can be defined [26] as:

$\sigma_{sf} = 0.45 * V_f * (\frac{L_f}{\phi}) * \sqrt{f'_c} = 0.4 * V_f * (\frac{L_f}{\phi}) * \sqrt{0.8 * 30} = 2.2 * V_f * (\frac{L_f}{\phi})$ (14).

Consequently, the tensile force can be calculated as: $T_{sf} = 2.2 * V_f * (\frac{L_f}{\phi}) * b * (t - \frac{a}{\beta 1})$ (15).

Based on the equilibrium equation and the previously mentioned equations, the nominal flexural moment can be calculated as:

$$M_n = [(A_s * F_s + A_f * F_f) * (d - \frac{a}{2}) + \sigma_{sf} * b * (t - c) * (\frac{t + c - a}{2})] \tag{16}$$

Eq. (16) for calculating the nominal flexural moment has been applied to a comprehensive set of 48 beam specimens, encompassing the seven beams from this research. The properties of the materials, geometric dimensions, reinforcement details, and steel fiber characteristics for all 48 beams are presented in Table 5. This table further includes both the experimentally obtained and nominal moment capacities for each beam specimen.

A meticulous examination of the tabulated results, coupled with a comparative analysis between the experimental and nominal flexural moments, reveals a consistent alignment. Notably, the assessment of nominal flexural strength yields predictions that consistently align with the experimental outcomes. The average ratio between the experimental and nominal flexural capacities stands at 1.05, with a standard deviation of 0.093.

In Fig. 13, a visual representation is provided to illustrate the comparative analysis between the experimental and nominal flexural capacities of the 48 beams under consideration. This graphical depiction serves to reinforce the reliability and consistency observed in the predictions derived from the nominal flexural strength assessment.

5. Conclusion

The study focused on the flexural performance of steel fiber-reinforced concrete beams employing a hybrid scheme (combining steel and GFRP reinforcement). The key findings derived from the experimental outcomes of the tested beams can be summarized as follows:

1) The presence of steel fibers (SF) in the concrete beams, reinforced with hybrid schemes, enhances ductility while simultaneously increasing load capacity and stiffness. This addresses the limitations associated with hybrid schemes and amplifies the advantages derived from the presence of GFRP. The experimental results underscore the effectiveness of combining hybrid schemes with steel fibers in RC beams.
2) Employing a hybrid scheme in concrete beams enhances load capacity, though it diminishes stiffness, ductility, and energy absorption. Specifically, there was a 27% and 25% decrease in stiffness for beams B2 and B3, featuring hybrid scheme ratios of 0.94% and 1.14%, respectively, compared to beam B1 with a 0.94% steel reinforcement ratio. Additionally, the toughness of beams B2 and B3 diminished by 7.4% and 13.2%, respectively, in comparison to beam B1.
3) The increase in the SF ratio also postponed the initiation of the first crack. The first crack load increased by 12.5% and 19% for beams with SF volumes of 0.50% and 1.00%, respectively. Also, as the SF volume ratio increased, the ultimate strain of GFRP bars also increased, resulting in an increased strain ductility of 13% and 22% for beams with SF volumes of 0.50% and 1.00%, respectively.
4) The enhancements in load capacity were 13% and 21% for beams with SF volumes of 0.50% and 1.00%, respectively. Likewise, the increase in stiffness measured 17% and 21% for beams with SF volumes of 0.50% and 1.00%, respectively. Furthermore, there was a rise in ductility factor by 65% and 132% for beams with SF volumes of 0.50% and 1.00%, respectively.
5) Significant agreement exists between experimental and predicted nominal flexural strength, affirming the efficiency of nominal flexural capacity as a successful predictor for SFRC beams reinforced with hybrid schemes. The nominal flexural strength of 48 tested beams, including those from this research, is closely aligned with experimental results, yielding an average ratio of 1.05.

CRediT authorship contribution statement

Ahmed El Bakzawy: Writing – original draft, Investigation, Funding acquisition, Formal analysis, Data curation. **T. S. Mustafa:** Writing – review & editing, Validation, Supervision, Methodology, Investigation, Conceptualization. **Mohamed H. Makhlouf:** Conceptualization, Investigation, Writing – review & editing. **Maher Adam:** Conceptualization, Supervision, Writing – review & editing.

Declaration of Competing Interest

The authors declare that they have no conflict of interest.

Data availability

Data will be made available on request.

References

[1] Adam MA, Said M, Mahmoud AA, Shanour AS. Analytical and experimental flexural behavior of concrete beams reinforced with glass fiber reinforced polymers bars. Constr Build Mater 2015;vol. 84:354–66. https://doi.org/10.1016/j.conbuildmat.2015.03.057.

[2] Pawłowski D, Szumigała M. Flexural behaviour of full-scale basalt FRP RC beams – experimental and numerical studies. Procedia Eng 2015;vol. 108:518–25. https://doi.org/10.1016/j.proeng.2015.06.114.
[3] Soric Z, Kisicek T, Galic J. Deflections of concrete beams reinforced with FRP bars. Mater Struct 2010;vol. 43(1):73–90. https://doi.org/10.1617/s11527-010-9600-1.
[4] Dong H-L, Zhou W, Wang Z. Flexural performance of concrete beams reinforced with FRP bars grouted in corrugated sleeves. Compos Struct 2019;vol. 215:49–59. https://doi.org/10.1016/j.compstruct.2019.02.052.
[5] Abed Farid, Alhafiz Abdul Rahman. Effect of basalt fibers on the flexural behavior of concrete beams reinforced with BFRP bars. 1 May Compos Struct 2019;Volume 215:23–34. https://doi.org/10.1016/j.compstruct.2019.02.050.
[6] Abed Farid, Sabbagh Mohamad Kusay, Karzad Abdul Saboor. Effect of basalt microfibers on the shear response of short concrete beams reinforced with BFRP bars. 1 August Compos Struct 2021;Volume 269:114029. https://doi.org/10.1016/j.compstruct.2021.114029.
[7] Xingyu G, Yiqing D, Jiwang J. Flexural behavior investigation of steel-GFRP hybrid-reinforced concrete beams based on experimental and numerical methods. Eng Struct 2020;vol. 206:110117. https://doi.org/10.1016/j.engstruct.2019.110117.
[8] Ruan X, Lu C, Xu K, Xuan G, Ni M. Flexural behavior and serviceability of concrete beams hybrid-reinforced with GFRP bars and steel bars. Compos Struct 2020;vol. 235:111772. https://doi.org/10.1016/j.compstruct.2019.111772.
[9] Zhou B, Wu R, Lu S, Yin S. A general numerical model for predicting the flexural behavior of hybrid FRP-steel reinforced concrete beams. Eng Struct 2021;vol. 239:112293. https://doi.org/10.1016/j.engstruct.2021.112293.
[10] Hasan MA, Akiyama M, Kashiwagi K, Kojima K, Peng L. Flexural behaviour of reinforced concrete beams repaired using a hybrid scheme with stainless steel rebars and CFRP sheets. Constr Build Mater 2020;vol. 265:120296. https://doi.org/10.1016/j.conbuildmat.2020.120296.
[11] El Refai A, Abed F, Al-Rahmani A. Structural performance and serviceability of concrete beams reinforced with hybrid (GFRP and steel) bars. Constr Build Mater 2015;vol. 96:518–29. https://doi.org/10.1016/j.conbuildmat.2015.08.063.
[12] Hawileh RA. Finite element modeling of reinforced concrete beams with a hybrid combination of steel and aramid reinforcement. Mater Des 2015;vol. 65:831–9. https://doi.org/10.1016/j.matdes.2014.10.004.
[13] Araba AM, Ashour AF. Flexural performance of hybrid GFRP-Steel reinforced concrete continuous beams. Compos Part B Eng 2018;vol. 154:321–36. https://doi.org/10.1016/j.compositesb.2018.08.077.
[14] Almahmood H, Ashour A, Sheehan T. Flexural behaviour of hybrid steel-GFRP reinforced concrete continuous T-beams. Compos Struct 2020;vol. 254:112802. https://doi.org/10.1016/j.compstruct.2020.112802.
[15] Sun Z, Fu L, Feng D-C, Vatuloka AR, Wei Y, Wu G. Experimental study on the flexural behavior of concrete beams reinforced with bundled hybrid steel/FRP bars. Eng Struct 2019;vol. 197:109443. https://doi.org/10.1016/j.engstruct.2019.109443.
[16] Said M, Shanour AS, Mustafa TS, Abdel-Kareem AH, Khalil MM. Experimental flexural performance of concrete beams reinforced with an innovative hybrid bars. Eng Struct 2021;vol. 226:111348. https://doi.org/10.1016/j.engstruct.2020.111348.
[17] Said M, Mustafa TS, Shanour AS, Khalil MM. Experimental and analytical investigation of high performance concrete beams reinforced with hybrid bars and polyvinyl alcohol fibers. Constr Build Mater 2020;vol. 259:120395. https://doi.org/10.1016/j.conbuildmat.2020.120395.
[18] Zhu H, Cheng S, Gao D, Neaz SM, Li C. Flexural behavior of partially fiber-reinforced high-strength concrete beams reinforced with FRP bars. Constr Build Mater 2018;vol. 161:587–97. https://doi.org/10.1016/j.conbuildmat.2017.12.003.
[19] Musmar M. Tensile strength of steel fiber reinforced concrete. Contemp Eng Sci 2013;vol. 6:225–37. https://doi.org/10.12988/ces.2013.3531.
[20] Saba AM, et al. Strength and flexural behavior of steel fiber and silica fume incorporated self-compacting concrete. J Mater Res Technol 2021;vol. 12:1380–90. https://doi.org/10.1016/j.jmrt.2021.03.066.
[21] Usman M, Farooq SH, Umair M, Hanif A. Axial compressive behavior of confined steel fiber reinforced high strength concrete. Constr Build Mater 2020;vol. 230:117043. https://doi.org/10.1016/j.conbuildmat.2019.117043.
[22] Liew KM, Akbar A. The recent progress of recycled steel fiber reinforced concrete. Constr Build Mater 2020;vol. 232:117232. https://doi.org/10.1016/j.conbuildmat.2019.117232.
[23] Blagojević P, Blagojević N, Kukaras D. Flexural behavior of steel fiber reinforced concrete beams: probabilistic numerical modeling and sensitivity analysis. Appl Sci 2021;vol. 11(20). https://doi.org/10.3390/app11209591.
[24] Abbass W, Khan MI, Mourad S. Evaluation of mechanical properties of steel fiber reinforced concrete with different strengths of concrete. Constr Build Mater 2018;vol. 168:556–69. https://doi.org/10.1016/j.conbuildmat.2018.02.164.
[25] Zhang P, Li Q, Chen Y, Shi Y, Ling Y-F. Durability of steel fiber-reinforced concrete containing SiO2 nano-particles. Materials 2019;vol. 12(13). https://doi.org/10.3390/ma12132184.
[26] Beshara FBA, Shaaban IG, Mustafa TS. Nominal flexural strength of high strength fiber reinforced concrete beams. Arab J Sci Eng 2012;vol. 37(2):291–301. https://doi.org/10.1007/s13369-012-0172-y.
[27] Chalioris CE, Kosmidou P-MK, Karayannis CG. Cyclic response of steel fiber reinforced concrete slender beams: an experimental study. Materials 2019;vol. 12(9). https://doi.org/10.3390/ma12091398.
[28] Nassani DE. Experimental and analytical study of the mechanical and flexural behavior of hybrid fiber concretes. Structures 2020;vol. 28:1746–55. https://doi.org/10.1016/j.istruc.2020.10.014.
[29] Lai MH, Lu ZY, Luo YT, Ren FM, Cui J, Wu ZR, Ho JCM. Pre- and post-fire behaviour of glass concrete from wet packing density perspective. J Build Eng 2024;Vol. 86. https://doi.org/10.1016/j.jobe.2024.108758.
[30] Huang ZC, Liu JJ, Ren FM, Cui a J, Song Z, Lu DH, Lai MH. Behavior of SSFA high-strength concrete at ambient and after exposure to elevated temperatures. Case Stud Constr Mater 2024;Vol. 20. https://doi.org/10.1016/j.cscm.2024.e02946.
[31] Lai MH, Lin JL, Cui J, Ren FM, Kitipornchai S, Ho JCM. A novel packing-coupled stress-strain model for confined concrete. Eng Struct 2024;Vol. 303. https://doi.org/10.1016/j.engstruct.2023.117415.
[32] Lai Mianheng, Hanzic Lucija, Ho Johnny CM. Fillers to improve passing ability of concrete. Struct Concr 2019;Vol. 20. https://doi.org/10.1002/suco.201800047.
[33] Suna Z, Fua L, Fenga D, Vatulokaa AR, Weib Y, Wu G. Experimental study on the flexural behavior of concrete beams reinforced with bundled hybrid steel/FRP bars. Eng Struct 2019;197.
[34] ACI Committee 318. Building Code Requirements for Structural Concrete (ACI 318-14) and Commentary (ACI 318R-14). Farmington Hills, MI: American Concrete Institute,; 2014.
[35] ISIS Canada. Reinforcing concrete structures with fiber reinforced polymers. ISIS-M03-07. Canadian Network of Centers of Excellence on Intelligent Sensing for Innovative Structures. Winnipeg, Man: Univ. of Winnipeg,; 2007.